Received: 5 May 2016 | Revised: 27 October 2016 | Accepted: 8 December 2016

DOI 10.1002/bio.3275

WILEY LUMINESCENCE
The Journal of Biological and Chemical Luminescence

RESEARCH ARTICLE

Probing the mechanism of interaction of metoprolol succinate with human serum albumin by spectroscopic and molecular docking analysis

Suma K. Pawar | **Seetharamappa Jaldappagari**

Department of Chemistry, Karnatak University, Dharwad, India

Correspondence
Seetharamappa Jaldappagari, Department of Chemistry, Karnatak University, Dharwad-580003, India.
Email: jseetharam@yahoo.com

Funding information
University Grant Commission, New Delhi, India for awarding the Rajiv Gandhi National Fellowship, Grant/Award Number: RGNF-2015-17-SC-KAR-11858

Abstract

In the present work, the mechanism of the interaction between a β1 receptor blocker, metoprolol succinate (MS) and human serum albumin (HSA) under physiological conditions was investigated by spectroscopic techniques, namely fluorescence, Fourier transform infra-red spectroscopy (FT-IR), fluorescence lifetime decay and circular dichroism (CD) as well as molecular docking and cyclic voltammetric methods. The fluorescence and lifetime decay results indicated that MS quenched the intrinsic intensity of HSA through a static quenching mechanism. The Stern–Volmer quenching constants and binding constants for the MS–HSA system at 293, 298 and 303 K were obtained from the Stern–Volmer plot. Thermodynamic parameters for the interaction of MS with HSA were evaluated; negative values of entropy change (ΔG°) indicated the spontaneity of the MS and HSA interaction. Thermodynamic parameters such as negative ΔH° and positive ΔS° values revealed that hydrogen bonding and hydrophobic forces played a major role in MS–HSA interaction and stabilized the complex. The binding site for MS in HSA was identified by competitive site probe experiments and molecular docking studies. These results indicated that MS was bound to HSA at Sudlow's site I. The efficiency of energy transfer and the distance between the donor (HSA) and acceptor (MS) was calculated based on the theory of Fosters' resonance energy transfer (FRET). Three-dimensional fluorescence spectra and CD results revealed that the binding of MS to HSA resulted in an obvious change in the conformation of HSA. Cyclic voltammograms of the MS–HSA system also confirmed the interaction between MS and HSA. Furthermore, the effects of metal ions on the binding of MS to HSA were also studied.

KEYWORDS

binding, fluorescence quenching, FRET, metoprolol succinate, molecular docking

1 | INTRODUCTION

When a drug enters the blood stream it binds to plasmatic proteins, namely serum albumin and glycoproteins. This drug–protein binding is reversible in nature in which an equilibrium exists between the bound and free drug molecule. Only the unbound fraction of the drug shows its therapeutic effects in the body. The degree of protein binding varies from drug to drug.[1] The protein binding tendency of a drug is considered to be the most significant factor when its pharmaceutical action is evaluated, as drug efficiency is affected by the degree to which it binds to serum proteins.[2] If drug-binding affinity towards serum protein is weak, then the drug will be metabolized and excreted from the body very quickly, so its therapeutic effect will be low. If the binding affinity of a drug is high then its retention time in the body will be high. This situation results in its toxicity and undesired side effects.[3] So, investigations on drug–protein binding help to determine the rate of absorption, distribution, metabolism and excretion of the drug in the body and to improve drug efficacy for better therapeutic effects.[4]

The major studied serum proteins are albumins [human serum albumin (HSA) and bovine serum albumin (BSA)] and globulins (α-, β- and γ-globulins). Among these, HSA is the major component of human

Abbreviations used: ATR, attenuated total reflection; BSA, bovine serum albumin; CD, circular dichroism; FRET, Fosters' resonance energy transfer; HSA, human serum albumin; MRE, mean residue ellipticity; MS, metoprolol succinate; NMR, nuclear magnetic resonance.

blood and constitutes about half of the proteins in the blood stream. It is mainly known for its multifunctional action. It serves as a transport protein for many exogenous, and endogenous ligands and drug molecules.[5] The globular heart-shaped protein consists of 585 amino acids with a molecular weight of 66 kDa. Three α-helical domains (I, II and III) are further divided into two subdomains (A and B).[6] Generally, ligands and drug molecules bind to HSA in its two principal regions located in hydrophobic cavities, namely subdomains IIA and IIIA called site I and site II, respectively.

Metoprolol succinate (MS), chemically known as (RS)-1-(isopropyl amino)-3-[4-(2-methoxyethyl)phenoxy]propan-2-ol succinate (Figure 1), is a β1-selective (cardioselective) adrenoceptor blocker.[7] It is extensively used in the treatment of hypertension, angina pectoris, arrhythmia, myocardial infarction, supraventricular tachycardia, congestive heart failure and also in the prevention of migraine headaches.[8,9] MS lowers the risk of heart attack by reducing the antagonistic effect of catecholamines on the heart that are released during physical and mental stresses.[10,11] Due to its selectivity in blocking the β1 receptors in the heart, metoprolol is also prescribed for off-label use in performance anxiety, social anxiety disorder, and other anxiety disorders. As with other pharmaceutical drugs, MS also has some common side effects that include trouble sleeping, tiredness, abdominal discomfort, abnormally low blood pressure, depression, dizzy and slow heartbeat.[12]

Numerous techniques, namely fluorescence spectroscopy,[13,14] ultraviolet–visible (UV–vis) light spectroscopy,[15] CD spectroscopy,[16] equilibrium dialysis,[17] electrochemical methods[18] and nuclear magnetic resonance (NMR) spectroscopy[19] have been employed to investigate drug–protein interactions. Among these, fluorescence spectroscopy is considered to be the best method to study drug–protein interactions due to its high sensitivity, rapidity and ease of implementation.[20] Mashiur et al.[21] have studied the binding of MS to BSA using an equilibrium dialysis method. They have investigated the effect of palmitic acid on the interaction of MS with BSA by determining the binding constant of the MS–BSA system in the presence or absence of palmitic acid. They have also determined the binding site for MS on BSA. However, they have not investigated the changes that may occur in the secondary structure of the protein upon interaction with MS.

A literature survey revealed that attempts have not been made so far to investigate the interaction of MS with HSA. This prompted us to explore the binding affinity of MS towards HSA in terms of binding constant, to recognize the specific binding site for MS on HSA, to determine the binding force acting between MS and HSA and also to examine the effect of binding of MS on the HSA secondary structure. The present study gives insights into the mechanism of interaction of MS with the transporter protein, HSA.

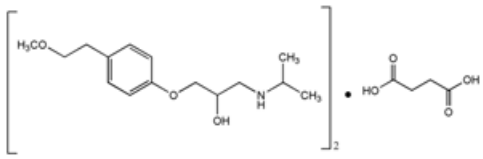

FIGURE 1 Structure of metoprolol succinate (MS)

2 | EXPERIMENTAL

2.1 | Reagents

HSA was purchased from the Sigma Chemical Company (St. Louis, MO, USA). A stock solution of HSA (100 μM) was prepared in phosphate buffer of pH 7.4 without any further purification. Metoprolol succinate was obtained as a gift sample from Reddy's Laboratories, India. A stock solution of MS (150 μM) was prepared in water. Phenyl butazone, ibuprofen and digitoxin were purchased from Sigma Chemical Company, Bangalore, India. Analytical grade chemicals and Millipore water were used in this study.

2.2 | Apparatus

Fluorescence measurements were performed on an Agilent Technologies Carry Eclipse fluorescence spectrophotometer equipped with a xenon flash lamp source and a Cary single cell peltier for temperature control. Both the excitation and emission slit widths were set at 5 nm. Fluorescence lifetime decay measurements were made on a Chronos BH time-resolved fluorescence lifetime spectrometer 90021 (ISS, USA). FT-IR spectra were recorded on a Nicolet Nexus 670 FT-IR spectrometer (USA) equipped with a germanium attenuated total reflection (ATR) piece. All spectra were recorded via the ATR method with a resolution of 4 cm^{-1} and 60 scans. Circular dichroism (CD) spectra were recorded on a Jasco J-715 spectropolarimeter (Tokyo, Japan) using a cell of 1 mm path length. Voltammetric measurements were performed on a CHI-1110a Electrochemical analyser (CH Instruments Ltd Co., USA, version 4.01).

2.3 | Fluorescence measurements

Fluorescence spectra of HSA in the presence or absence of MS were recorded in the range 300–500 nm upon excitation of HSA at 295 nm at different temperatures (293, 298 and 303 K). The concentration of HSA was fixed at 4.16 μM, while that of MS was varied from 6 to 60 μM.

2.4 | Displacement studies

Three different well known site probes, namely phenylbutazone (site I), ibuprofen (site II) and digitoxin (site III) were used in displacement studies. For this part of the study, the experiment was performed by keeping both HSA and site probe concentration constant (4.16 μM) and by varying the concentration of MS (6–60 μM).

2.5 | Effects of metal ions

Fluorescence emission spectra of MS–HSA system in the presence or absence of Cu^{2+} and Zn^{2+} ions were recorded separately, by keeping the concentration of HSA and metal ion at 4.16 μM and by varying the concentration of MS (6–60 μM).

2.6 | Fluorescence lifetime measurements

Fluorescence lifetime of HSA was recorded in the presence of increasing concentrations of MS upon excitation of HSA at 290 nm. The

goodness of fit was estimated using χ^2 values. For this study, [HSA] = 4.16 μM and [MS] = 6–36 μM.

2.7 | 3D–Fluorescence studies

The 3D–fluoresence spectra of HSA (4.16 μM) were recorded in the presence or absence of MS (48 μM) in the range 200–350 and 200–550 nm for excitation and emission wavelength, respectively.

2.8 | FT-IR spectroscopic studies

The FT-IR spectra of HSA (4.16 μM) were recorded in the presence or absence of MS in the range of 1300–1800 cm^{-1} at pH 7.4.

2.9 | Circular dichroism spectra

CD spectra of HSA in the presence of different concentrations of MS were recorded in the range of 200–260 nm at room temperature. The concentration of HSA was kept constant (4.16 μM) and that of MS was varied. The molar ratio of HSA to MS was 1:0, 1:3, 1:6, 1:9 or 1:12.

2.10 | Voltammetric studies

Differential pulse voltammograms of MS in the presence or absence of HSA were recorded in phosphate buffer pH 7.4 in the potential range 0.9–1.80 V. To the fixed concentration of MS, increased amounts of HSA were added and the corresponding voltammograms were recorded.

2.11 | Molecular docking studies

Blind docking between MS and HSA was performed using MGL tools with 1.5.4 with AutoGrid 4 and AutoDock 4. HSA (PDB id 1AO6) was obtained from the Protein Data Bank. The ligand (MS) PDB was developed using the Discovery Studio program. Docking calculations were performed employing Lamarckian genetic algorithms and keeping all other parameters as default settings. After docking, low energy docked conformation was selected that was then visualized using PyMol software.

3 | RESULTS AND DISCUSSION

3.1 | Steady-state fluorescence measurements

The amino acid residue (tryptophan), which is responsible for intrinsic fluorescence intensity of serum proteins, is sensitive to the changes in its microenvironment upon binding of small molecules to serum protein.[22,23] Therefore, fluorescence quenching measurements are widely performed to explore drug–protein interactions in which the decrease in fluorescence intensity of the protein in the presence of a drug is considered as an indication of drug–protein binding.[24] Thus, in order to understand the molecular interaction between MS and HSA, we have carried out fluorescence measurements. The effect of MS on the intrinsic intensity of HSA was studied by recording HSA fluorescence spectra in the presence or absence of MS in phosphate buffer pH 7.4. When HSA was excited at 295 nm, it exhibited an intense emission peak at 342 nm. On subsequent addition of MS to HSA, a decrease in the HSA emission intensity was observed along with a shift in its emission wavelength from 342 nm to 338 nm (Figure 2). The blue shift observed was attributed to increased polarity around the tryptophan upon binding of MS to HSA.[25] These observations revealed the interaction between MS and HSA.

Quenching of fluorescence intensity of protein by ligands or drug molecules occurs mainly by two different mechanisms, namely dynamic and static quenching. Dynamic quenching results from collisions between a fluorophore and a quencher at the excited state whereas static quenching results from the non-fluorescent ground state complex formation between a fluorophore and a quencher.[22,26] These two quenching mechanisms can be differentiated by the difference in their dependence on temperature. In dynamic quenching mechanisms, higher temperatures result in faster diffusion of protein and drug molecules and hence the amount of collision quenching constant increases. But for static quenching mechanisms, a higher temperature reduces the stability of the non-fluorescent complex formed at the ground state and thus the static quenching constant decreases.[27]

The plausible quenching mechanism for MS–HSA interaction was established by recording the HSA fluorescence spectra in the presence or absence of MS at 293, 298 and 303 K. The results obtained were analysed using the Stern–Volmer equation shown below:

$$Fo/F = 1 + K_q T_o[Q] = 1 + K_{sv}[Q] \quad (1)$$

where Fo and F are the fluorescence intensities in the presence or absence of the quencher, K_q is the bimolecular quenching constant ($K_q = K_{sv}/T_o$), T_o is the average lifetime of the fluorophore in the absence of quencher (in nsec), [Q] is the concentration of the quencher and K_{sv} is the Stern–Volmer quenching constant.[28] The Stern–Volmer plots for HSA in the presence or absence of MS at 293, 298 and 303 K are shown in Figure 3. The K_{sv} and K_q values were calculated from the slope of Fo/F versus [Q] plot at different temperatures and are listed in Table 1.

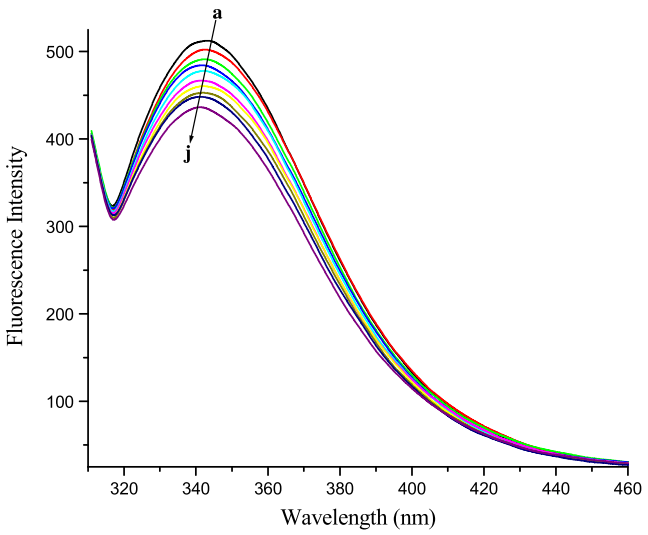

FIGURE 2 Fluorescence quenching of HSA by MS; [HSA = 4.16 μM] (a), MS = 6, 12, 18, 24, 30, 36, 42, 48, 54 and 60 μM (b–j)

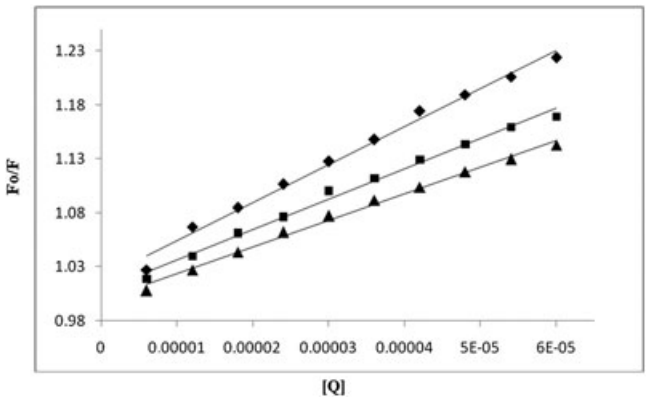

FIGURE 3 The Stern–Volmer plot for the binding of MS–HSA at 293 [♦], 298 [▪] and 303 [▴]K

It is evident from the results shown in Table 1 that the K_{sv} values decreased with increase in temperature indicating the formation of the MS–HSA complex at the ground state. Furthermore, the K_q values were found to be greater than 10^{10} M^{-1} sec^{-1} suggesting the presence of a static quenching mechanism.[22] In view of the above, we have proposed that MS quenched the fluorescence intensity of HSA through a static quenching mechanism in the present study.

3.2 | Evaluation of binding and thermodynamic parameters for MS–HSA system

There are n equivalent and independent binding sites available on the protein for the binding of small molecules.[29] When small molecules bind to this set of equivalent binding sites of protein, the binding constant (K_b) and the number of binding sites (n) can be determined using the equation given below[30]:

$$\log[(Fo-F)/F] = \log K + n \log[Q] \quad (2)$$

where K is the binding constant and n is the number of binding sites per HSA molecule. The intercept and slope of the plot of log [Fo - F/F] versus log[Q] correspond to K and n values respectively. The values of K and n for the MS–HSA complex at 298 K were determined and are given in Table 1. The binding constants decreased with increase in temperature suggesting the decreased stability of the MS–HSA complex at higher temperatures. The values of n close to unity indicated the existence of a single binding site for MS on HSA.

Protein–ligand interactions are held by major forces that play a significant role in their interactions. These include electrostatic interactions, hydrogen bond, van der Waals interactions and hydrophobic interactions.[31,32] The depiction of temperature-dependent thermodynamic parameters (ΔG°, ΔH° and ΔS°) help in determining the forces responsible for protein–ligand interactions. Thermodynamic parameters were therefore determined for the MS–HSA system at different temperatures to characterize the binding force acting between MS and HSA using the van 't Hoff and Gibbs free energy equations shown below:

$$\log K = -\Delta H°/2.303RT + \Delta S°/2.303R \quad (3)$$

$$\Delta G° = -2.303\ RT \log K \quad (4)$$

where K is the binding constant and R is the gas constant. The values of ΔH° and ΔS° were obtained from the slope and intercept of the log K versus 1/T plot and the corresponding values are summarized in Table 1. The negative values of ΔG° showed that the interaction between MS and HSA was spontaneous. The negative ΔH° and positive ΔS° values revealed that hydrophobic forces play a major role in the MS–HSA interaction and stabilized the complex.[33,34]

3.3 | Identification of binding site for MS in HSA by site probe

Majority of drug molecules/ligands bind to HSA primarily at two Sudlow's sites, namely site I and site II located within subdomain IIA and IIIA respectively. Site probe studies help in identifying the specific binding site for the drug on the protein. This is carried out by monitoring the variation in the binding affinity between the drug and protein in the presence of the site probe.[35] So, in order to locate the binding site for MS on HSA, we have carried out site probe displacement studies using well known site probes, namely phenylbutazone, ibuprofen and digitoxin that are known to bind site I, site II and site III, respectively.[36,37] For this, increased concentrations of MS were added to equimolar solutions of HSA and site probe and fluorescence spectra were recorded. The results were analysed and binding constants were calculated from the slope of the plot of log[Fo - F/F] versus log[Q]. Binding constants of MS–HSA system at 298 K in the presence and absence of site probes are given in Table 2. The change in the binding constant of MS–HSA complex was negligible in the presence of ibuprofen and digitoxin, but significant change in its value was observed in the presence of phenylbutazone. This indicated that both phenylbutazone and MS compete for site I in HSA and further, phenylbutazone was displaced by MS from HSA. These results suggested that site I was the binding site for MS on HSA.[38]

3.4 | Time-resolved fluorescence measurements

The time-resolved fluorescence spectroscopic technique is widely used to investigate the mechanism of quenching in drug–protein interactions. It is the best method to distinguish between static and

TABLE 1 Stern–Volmer quenching constants, bimolecular quenching constants, binding constants, number of binding sites and thermodynamic parameters for MS–HSA interaction at different temperatures

T (K)	K_{sv} (L mol^{-1})	K_q (L mol^{-1} sec^{-1})	K (M^{-1})	n	R^2	ΔH° kJ mol^{-1}	ΔS° J K^{-1} mol^{-1}	ΔG° kJ mol^{-1}
293	3.32×10^3	3.32×10^{11}	33.3×10^4	1.00	0.99			-17.2
298	2.87×10^3	2.87×10^{11}	3.80×10^3	1.00	0.98	-595.47	+82.64	-19.8
303	2.53×10^3	2.53×10^{11}	1.53×10^3	1.02	0.99			-24.4

TABLE 2 Comparison of binding constants of MS–HSA system in the presence of site probes at 298 K

System	Without site probe K (M^{-1})	Phenyl butazone K (M^{-1})	Ibuprofen K (M^{-1})	Digitoxin K (M^{-1})
MS–HSA	3.80×10^3	2.53×10^3	3.76×10^3	3.65×10^3

dynamic quenching mechanism.[26] In dynamic quenching, the collision between the fluorophore and quencher in the excited state decreases the lifetime of fluorophore, while in the static quenching mechanism the complex is formed at ground state only and hence, there will not be any change over the lifetime of the complex.[28] Therefore, to examine the quenching mechanism existing in MS–HSA binding, we have performed time-resolved fluorescence measurements. The time-resolved fluorescence decay curve of HSA was recorded in the presence or absence of different concentrations of MS. The fluorescence decay curves of HSA were fitted as triexponential.[39] The fluorescence decay parameters for HSA in the presence or absence of MS are shown in Table 3. No significant change in the average lifetime of HSA was observed in the presence of MS. This observation ruled out the possibility of dynamic quenching mechanism. Hence, it was confirmed that MS quenched the intensity of HSA through a static quenching mechanism.[40,41]

3.5 | Characterization of interaction of MS–HSA by FT-IR spectroscopy

Fourier transform-infrared spectroscopy is an excellent technique to explore the secondary structure of proteins and also to investigate the change in protein secondary structure upon drug binding.[42] The FT-IR spectrum of a protein exhibits two characteristic amide bands, namely amide I and amide II. These two amide bands are the prominent vibrational bands of the protein backbone.[43] Amide I band arises due to C = O stretching vibrations of the peptide linkage that appear in the region of 1700–1600 cm^{-1} while the amide II band is attributable to a C–N stretch coupled with an N–H bending mode that appears at 1600–1500 cm^{-1}. Both these amide bands are closely associated with the secondary structure of the protein. Among these two bands, the amide I band is more sensitive compared with the amide II band.[44] To explore the changes in the secondary structure of HSA upon its binding with MS, the FT-IR spectra of HSA in the presence or absence of MS were recorded and are displayed in Figure 4. In free HSA, amide I and amide II bands were observed at 1655 and 1542 cm^{-1} respectively. In the presence of MS, the amide I band was shifted from 1655 to 1652 while amide II band was shifted from 1542 to 1546 cm^{-1}. The change in the peak position of amide bands indicated that MS interacted with C = O groups in HSA. This resulted in the rearrangement of the polypeptide carbonyl hydrogen bonding pattern and thus changed the secondary structure of HSA.[45] Furthermore, the intensity of amide bands was decreased in the presence of MS. This was attributed to the loss of the HSA α-helical structure upon MS binding.[42] These observations suggested that MS binding induced changes in the HSA secondary conformation.

3.6 | Energy transfer from HSA to β-blocker

Förster resonance energy transfer (FRET) was extensively used to measure the distance of separation between a donor and an acceptor.[46] According to FRET, the efficiency of energy transfer, E between HSA (Trp-214) and MS can be measured using the following equation:

$$E = 1 - F/F_o = R_o^6/(R_o^6 + r^6) \quad (5)$$

where E is the efficiency of energy transfer and F and Fo are the fluorescence intensities of the donor in the presence or absence of the acceptor, respectively, r is the average distance between donor and acceptor and Ro is the critical distance at which the efficiency of energy transfer is 50%. R_o can be calculated using the expression given below:

$$R_o^6 = 8.8 \times 10^{-25} k^2 N^{-4} \Phi J \quad (6)$$

where k^2 is the spatial orientation factor, n is the refractive index of the medium, Φ is the fluorescence quantum yield of the donor and J is the overlap integral of emission spectrum of donor and absorption spectrum of acceptor. The J value can be determined using the following equation:

$$J = \Sigma F(\lambda)\, \varepsilon(\lambda)\, \lambda^4\, \Delta\lambda / \Sigma F(\lambda)\, \Delta\lambda \quad (7)$$

where F(λ) is the fluorescence intensity of the donor of wavelength λ, ε is the extinction coefficient of acceptor at λ. For HSA, k^2, N and Φ are reported as 2/3, 1.336 and 0.118 respectively.[47] The spectral overlap between fluorescence spectrum of HSA and absorption spectrum of MS is shown in Figure 5. By using the above equations, the E, J, R_o and r values for the MS–HSA system were calculated to be 0.11, 4.84×10^{-16} cm^3 L mol^{-1}, 1.48 nm and 1.12 nm, respectively. The

TABLE 3 Fluorescence lifetime decay of HSA in the presence of different concentrations of MS

	T_1	T_2	T_3	α_1	α_2	α_3	χ^2	<J > nsec
HSA (4.16 μM)	5.7	1.4	291	17.5	24.3	-0.11	1.18 2	2.39
MS 6 (μM)	6.02	1.67	143	16.6	26.1	-0.30	1.15	2.36
12	5.9	1.14	131	12.5	25.9	-0.10	1.11	2.34
18	5.72	1.5	312	17.5	24.4	-0.12	1.13	2.41
24	1.87	0.53	5.58	12.9	7.8	12.8	1.17	2.48
30	5.57	1.43	205	18	23.9	-0.17	1.23	2.40
36	1.69	0.32	5.44	14	9.65	13.4	1.26	2.49

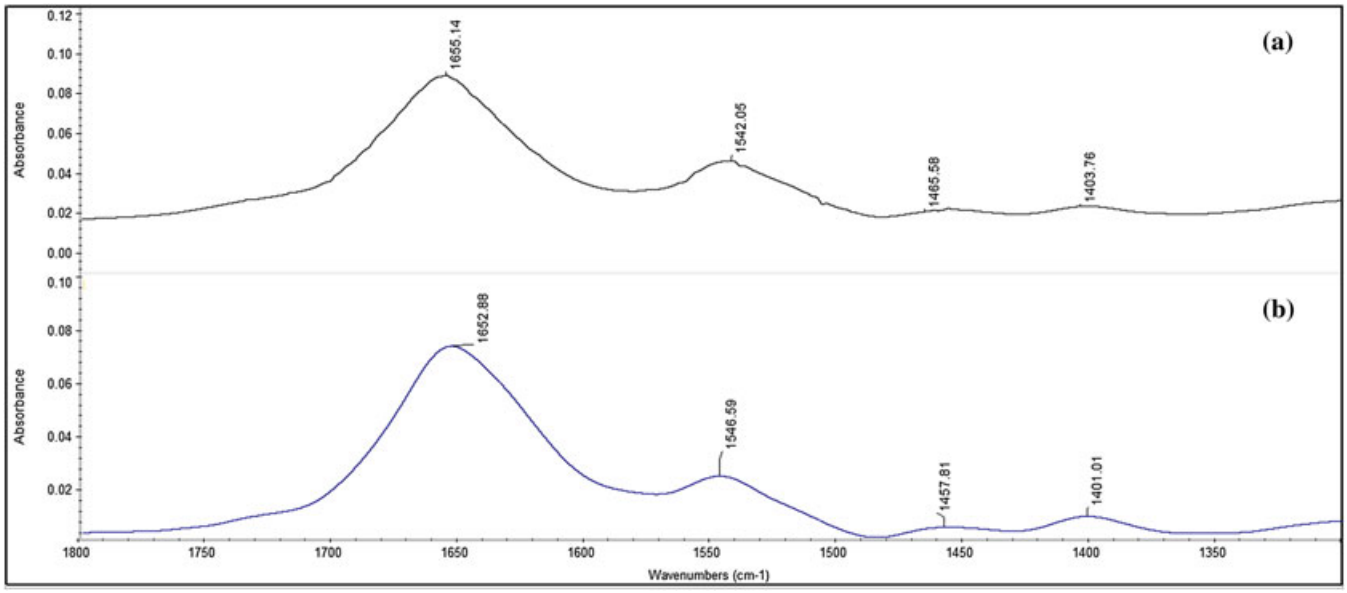

FIGURE 4 FT-IR spectra of free HSA (a) and MS-bound HSA (b)

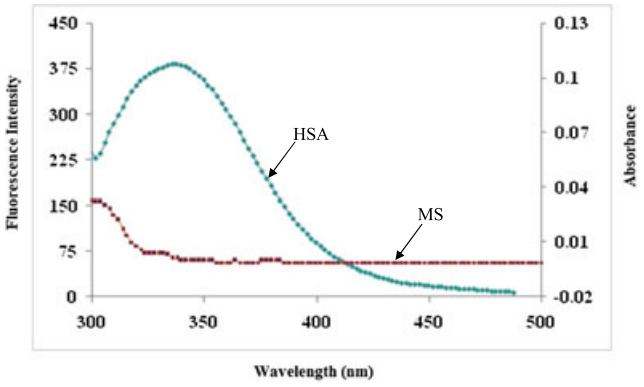

FIGURE 5 Overlap of UV absorption spectrum of MS with fluorescence emission spectrum of HSA

smaller value of r (less than 8 nm) indicated the high probability of energy transfer from HSA to MS.

3.7 | Effect of metal ions on MS–HSA binding

Many bivalent trace metal ions are present in the human body that play important functional roles in proteins.[48] These metal ions may affect the binding of the serum protein to the drug. Hence, the influence of Cu^{2+} and Zn^{2+} on MS–HSA binding was investigated. For this, the fluorescence spectra of the MS–HSA complex were recorded at 298 K before or after the addition of Cu^{2+} and Zn^{2+} separately. Binding constants of the MS–HSA complex were calculated in the presence or absence of Cu^{2+} and Zn^{2+}. It was found that the binding constant of MS–HSA decreased from 3.75×10^3 to 2.48×10^3 M^{-1} in the presence of Cu^{2+} while it increased to 4.50×10^3 M^{-1} in the presence of Zn^{2+}. The complexation of Cu^{2+} with protein reduced the binding affinity of MS to HSA and increased the availability of free MS in the blood. However, in the presence of Zn^{2+} the binding affinity between MS and HSA increased, which prolonged the storage time of MS in the blood plasma and hence its efficiency was enhanced in the body.[29]

3.8 | 3D fluorescence spectral study

3D–Fluorescence spectroscopy is a powerful tool to study the secondary conformational changes in the protein upon binding. In order to examine the effect of MS binding on the HSA secondary structure, 3D fluorescence spectra of HSA were recorded before or after the addition of MS. 3D–Fluorescence spectra and the corresponding contour spectra of free and MS-bound HSA are shown in Figure 6(a, b), respectively. HSA exhibited four typical peaks; among four peaks, 'a' is the Rayleigh scattering peak ($\lambda_{em} = \lambda_{ex}$), 'b' is the second order scattering peak ($\lambda_{em} = 2\lambda_{ex}$), and '1' and '2' are the fluorescence peaks that occur due to Tyr/Trp residues and polypeptide backbone respectively.[19] It was observed from the figure that upon MS addition, the intensity of both fluorescence peaks of HSA decreased with a blue shift in emission wavelength indicating conformational and microenvironmental changes around HSA induced by MS. Furthermore, the increase in intensity of the Rayleigh scattering peak in the presence of MS revealed the formation of the MS–HSA complex.[49]

3.9 | Conformational investigations

Circular dichroism is a well known and important technique to characterize the secondary structure of a protein and to study the effect of binding of a ligand on HSA secondary structure.[50,51] For this, we investigated the effect of MS binding on HSA secondary structure by recording HSA CD spectra in the presence of different concentrations of MS and the resulting spectra are displayed in Figure 7. The HSA CD spectrum exhibited two negative bands at 208 and 222 nm in UV region which are characteristic of α-helicity of the protein due to $n \rightarrow \pi^*$ transition in the peptide bond of the α-helix structure.[52]

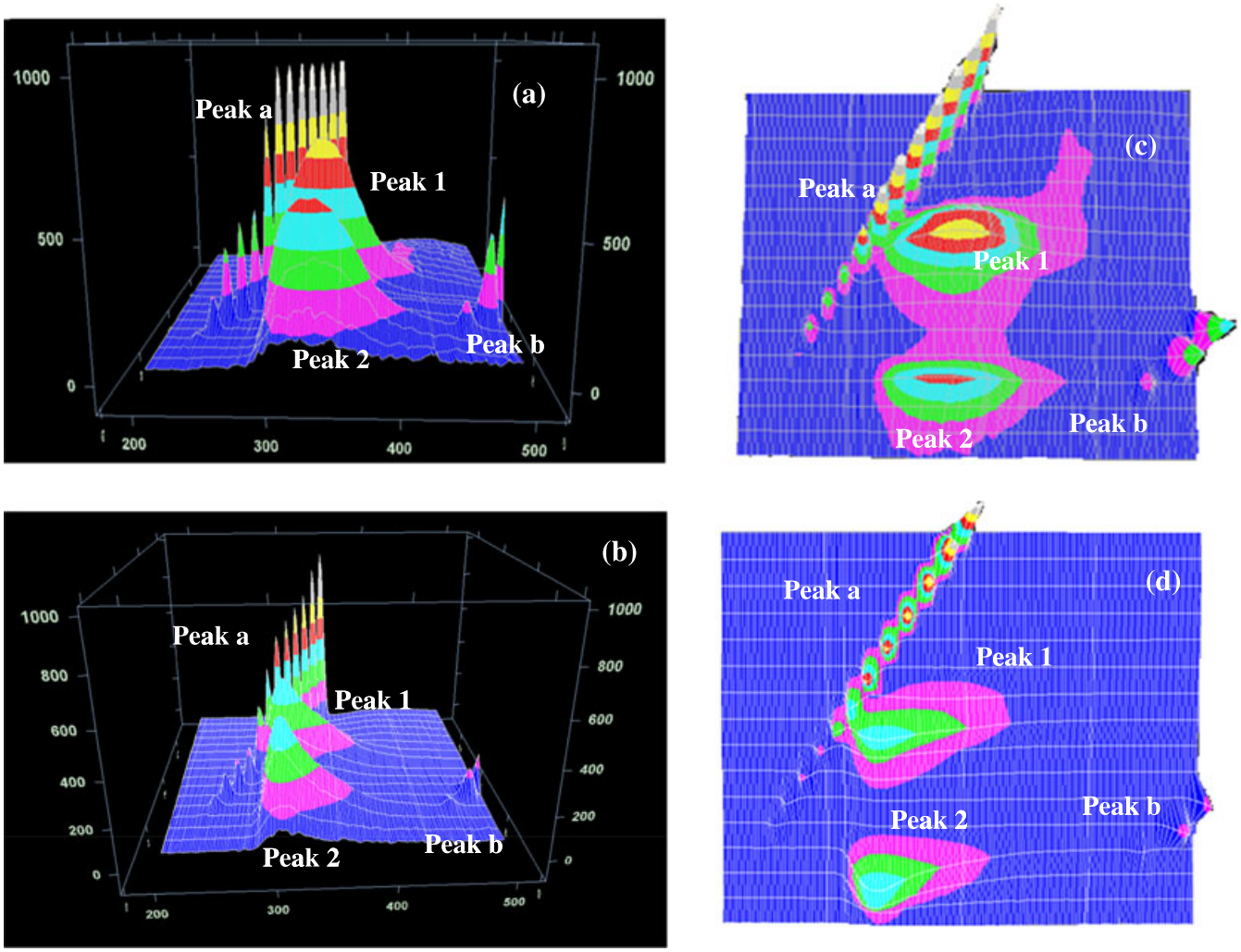

FIGURE 6 3D–Fluorescence spectra of HSA (a) and MS–HSA (b), and contour diagrams of HSA (c) and MS–HSA (d)

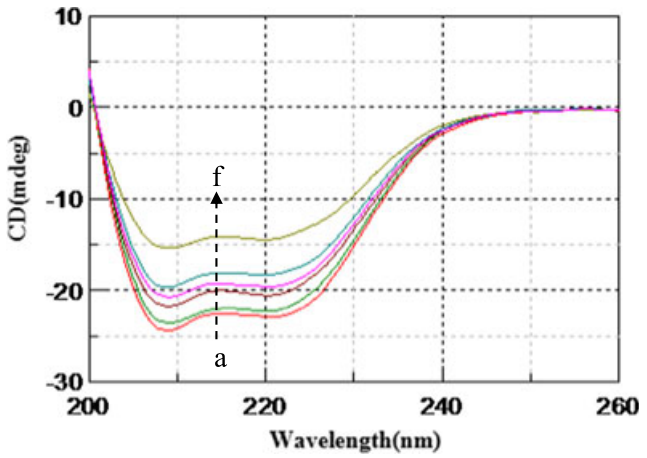

FIGURE 7 CD spectra of HSA (4.16 μM) (a); in the presence of 6 (b), 12 (c), 18 (d), 24 (e) and 30 μM (f) MS

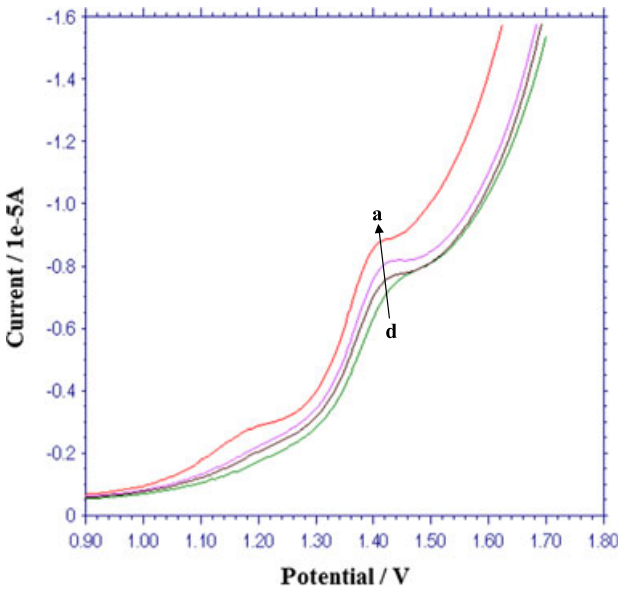

FIGURE 8 Differential pulse voltammograms of 60 μM MS (a) in the presence and absence of HSA (b–d; 2.5–7.5 μM)

The intensity of HSA CD signal was found to be increased regularly upon successive addition of MS without any shift in the peak wavelength. CD results are expressed in terms of mean residue ellipticity (MRE) in deg cm^2 $dmol^{-1}$ according to the following equation:

$$\text{MRE} = \text{observed CD (mdeg)}/\text{Cpnl}\times 10 \quad (8)$$

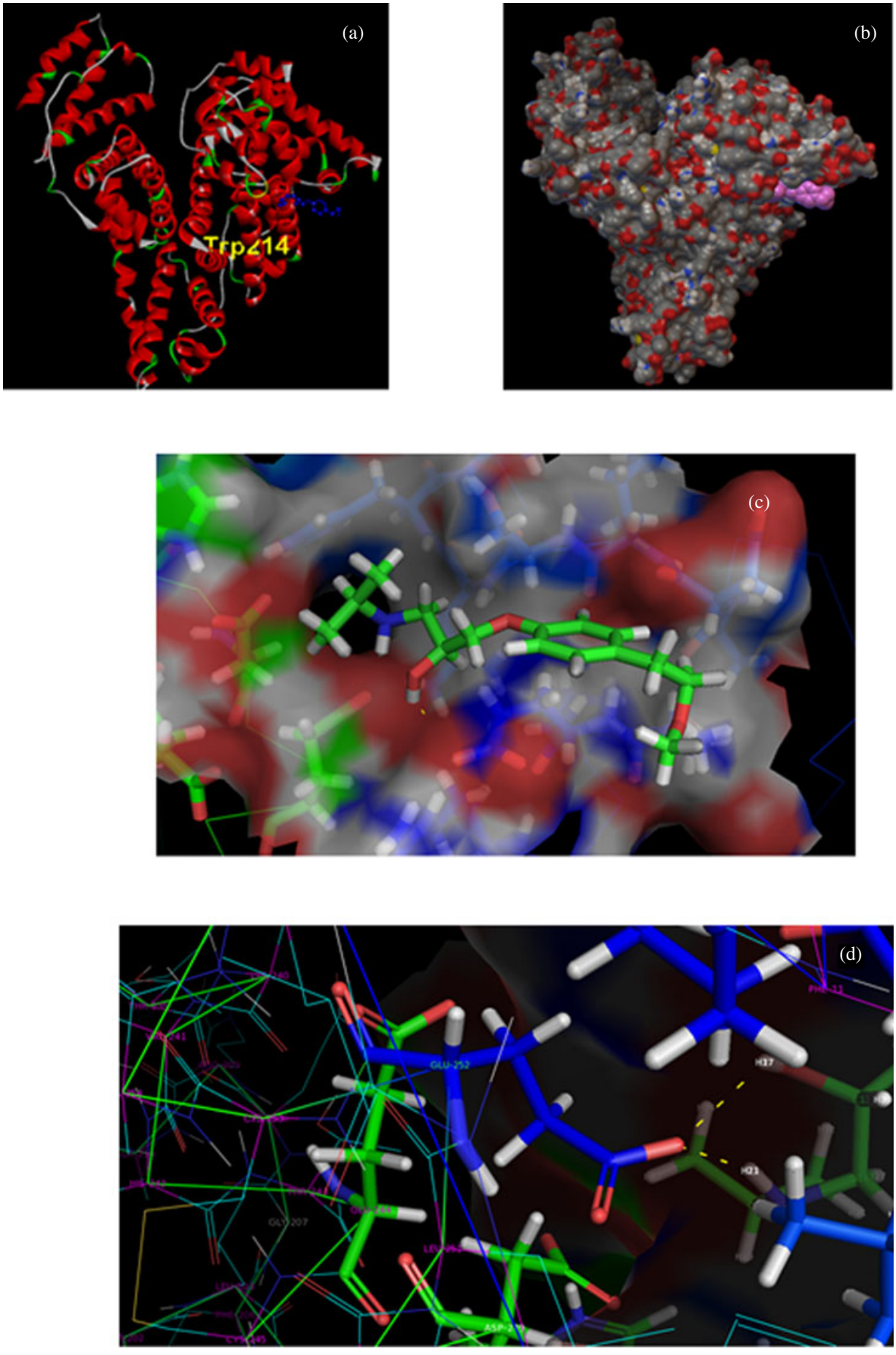

FIGURE 9 Molecular docking results of HSA complexed with MS. (a) MS bound to HSA at site I, (b) surface view of docked model of HSA with MS, (c) MS burried in the hydrophobic pocket of HSA and (d) stick model of MS–HSA system showing hydrogen bonding and surrounding amino acid residues

where CP is the molar concentration of the protein, n is the number of amino acid residues and l is the path length. The α-helical content of free HSA and MS-bound HSA was calculated from MRE values at 208 nm using the following equation:

$$\alpha\text{-helix}\ (\%) = [(-\mathrm{MRE}_{208} - 4000)/33\,000 - 4000] \times 100 \qquad (9)$$

where MRE_{208} is the observed MRE value at 208 nm, 4000 is the MRE of the β-form and random coil conformation cross at 208 nm and 33,000 is the MRE value of pure α-helix at 208 nm. By using equation 9, we have calculated the α-helical content of HSA in the presence and absence of MS and found to be decreased from 65.80% (in free HSA) to 59.65% (in MS-bound HSA). These results indicated that the binding of MS induced conformational changes in HSA.

3.10 | MS–HSA binding by voltammetric studies

Interaction between MS and HSA was characterized by the voltammetric technique. Differential pulse voltammograms of MS in the presence or absence of HSA are shown in Figure 8. MS exhibited an oxidation peak at 1.4 V at the glassy carbon electrode.

Upon the subsequent addition of HSA to MS solution, a decreased peak current of oxidation peak was observed with a slight shift in the peak potential. Decreased peak current of MS upon the addition of HSA revealed the interaction between MS and HSA and formation of a non-electroactive complex, MS–HSA, on the electrode surface.

3.11 | Exploring binding of MS to HSA by molecular docking

A molecular docking study helps in predicting the conformations and binding affinities of small molecules to proteins. In molecular docking, the entire surface of the protein was searched to find out the specific binding site for the ligand and simultaneously optimized the conformation of peptides. So, for the docking study it was considered to be important to understand the effective functioning of drug in the body.[41] By using the AutoDock 4.2 software package, MS was docked with HSA (PDB id: 1AO6) which generated 10 different docked model conformations. Out of the 10 different conformations, the best docked model of MS and HSA with lowest binding energy was selected and that conformation was used for further analysis. The docking results showed that MS was bound to HSA at the hydrophobic pocket of site I in subdomain IIA (Figure 9a–c). The hydrophobic pocket was surrounded by amino acid residues, namely, Leu-203, Gly-207, Glu-244, His-242, Cys-253, Phe-203, Val-241, Arg-209, Thr-239, Phe-206, Leu-251, Asp-219, Cys-245, Thr-243 and Lys-240. This indicated that hydrophobic interactions were predominant in the binding of MS to HSA (Figure 9d). MS was bound to HSA thorough two hydrogen bonds; one hydrogen bond was found in between Glu-252 and hydrogen atom (H17) of hydroxyl group attached to C-2 carbon with a bond distance of 1.8 nm and the second hydrogen bond was noticed in between Glu-252 and hydrogen (H21) attached to nitrogen of isopropyl amino group with a bond distance of 2.2 nm. These hydrogen bonds formed between the amino acid residues of protein and MS increased the hydrophobicity around the hydrophobic cavity to stabilize the MS–HSA complex. These results are observed to be in good agreement with the thermodynamic results. The binding energy and binding constant of MS–HSA system were found to be 16.10 kJ M^{-1} and 6.6 × 10^2 M^{-1} respectively, which are different from those obtained by fluorescence method. The probable reason for this could be the difference in X-ray structure of the protein in crystals and that of the aqueous system used in the study. This results in a different microenvironment around the ligand. Similar results are reported in HSA binding to different ligands.[30,53,54] The results of the site probe experiment were found to be in agreement with docking studies.

4 | CONCLUSION

In the present study, the mechanism of binding between MS and HSA, binding affinity, effect of metal ions on MS–HSA binding and the effect of MS binding on the secondary structure of HSA were explored for the first time by spectroscopic, voltammetric and molecular docking studies. The results of temperature studies and lifetime measurement studies revealed that MS quenched HSA intensity through a static quenching mechanism by binding it at site I in the subdomain IIA. Based on thr thermodynamic parameters of the MS–HSA interaction, we have proposed that hydrogen bonding and hydrophobic forces stabilized the MS–HSA complex. The Cu(II) ion decreased the binding affinity between MS and HSA, whilst Zn(II) enhanced the binding affinity. The change in HSA secondary structure upon interaction with MS was evident from 3D–fluoresence and CD studies.

ACKNOWLEDGMENTS

The authors thank the University Grant Commission, New Delhi, India for providing the financial support to carry out this work [F. No 43–205/2014(SR) dated 18 August 2015]. Thanks are due to the Chairman, Department of Molecular Biophysics, Indian Institute of Science, Bangalore, for CD facilities. One of the authors (Suma K. Pawar) acknowledges the University Grant Commission, New Delhi, India for awarding the Rajiv Gandhi National Fellowship (F1-17.1/2016–17/RGNF-2015-17-SC-KAR-11858).

REFERENCES

[1] C. Ràfols, S. Zarza, E. Bosch, *Talanta* **2014**, *130*, 241.

[2] Z. Hua-xin, X. Hang-xing, L. Li-wei, *Spectrochim Acta A* **2016**, *16*, 88.

[3] M. L. Hall, W. L. Jorgensen, L. Whitehead L, *J. Chem. Inf. Model.* **2013**, *53*, 907.

[4] H. Xu, N. Yao, H. Xu, T. Wang, G. Li, Z. Li, *Int. J. Mol. Sci.* **2013**, *14*, 14185.

[5] J. M. Berg, J. L. Tymoczko, L. Stryer, *Biochemistry*, 5th ed., New York **2002**.

[6] T. Peters Jr., *All about Albumins, Biochemistry, Genetics, and Medical Applications*, 1st ed., Academic Press, San Diego **1996**.

[7] G. D. Vaijanath, B. S. Sweta, P. K. Pravin, P. Manisha, K. J. Vivek, *J. Pharm. Biomed. Anal.* **2008**, *46*, 583.

[8] V. Gaikwad, *J. Pharm. Res.* **2010**, *3*, 788.

[9] J. Jaiswal, S. P. Anantawar, M. R. Narkhede, S. V. Gore, K. Mehta, *J. Pharm. Pharm. Sci.* **2012**, *4*, 96.

[10] D. Gabriela, C. Cecilia, E. Bodoki, H. Veronica, S. Alina, P. Elisabeth-Jeanne, S. F. Robert, *Farmacia* **2010**, *58*, 430.

[11] S. A. Pagar, D. M. Shinkar, R. B. Saudagar, *Int. J. Pharm. Biol. Sci.* **2013**, *3*, 224.

[12] https, //en.wikipedia.org/wiki/Metoprolol.

[13] S. Jie-hua, P. Dong-qi, W. Xiou-xiou, L. Ting-Ting, J. Min, W. Qi, *J. Photochem. Photobiol. B Biol.* **2016**, *162*, 14.

[14] Y. Yuanyuan, S. Yangyang, Y. Xuyang, L. Jianming, Z. Shufang, Z. Jia, *Chemosphere* **2016**, *161*, 475.

[15] H. Zhang, E. Liu, *J. Lumin.* **2014**, *153*, 182.

[16] J. Fahimeh, S. D. Parisa, M. Hamid, *J. Lumin.* **2014**, *148*, 347.

[17] M. Tanaka, Y. Asahi, S. Masuda, *J. Macromol. Sci. Part A Pure Appl. Chem.* **1995**, *32*, 339.

[18] C. Q. Xiao, F. L. Jiang, B. Zhou, R. Li, Y. Liu, *Photochem. Photobiol. Sci.* **2011**, *10*, 1110.

[19] L. S. Andria, S. L. Jennifer, *J. Pharm. Sci.* **2008**, *97*, 4670.

[20] K. B. Bahar, T. Sibel, D. Osman, *J. Lumin.* **2014**, *155*, 198.

[21] M. Rahman, P. Farzana, S. Mohammad, A. M. Mohammad, *Adv. Pharm. Bull.* **2014**, *4*, 379.

[22] Y. Yuanyuan, L. Jianming, L. Ren, S. Yangyang, L. Xiaoge, F. Jing, *Food Chem. Toxicol.* **2014**, *71*, 244.

[23] B. X. Huang, H. Y. Kim, C. Dass, *J. Am. Soc. Mass Spectrom.* **2004**, *15*, 1237.

[24] M. R. Eftink, C. A. Ghiron, *Anal. Biochem.* **1981**, *114*, 199.

[25] R. T. Mohammad, S. Hira, U. K. Asad, *Mol. Pharmaceutics* **1785**, *2014*, 11.

[26] J. R. Lakowicz, *Principles of Fluorescence Spectroscopy* 2nd ed, Springer, New York **2006**.

[27] Y. Yuanyuan, L. Jianming, L. Ren, D. Qiao, F. Jing, *Spectrochim. Acta A* **2014**, *124*, 46.

[28] L. Jianming, Y. Yuanyuan, W. Jing, Y. Xuyang, L. Ren, S. Yangyang, L. Xiaoge, *Spectrochim. Acta A* **2015**, *145*, 473.

[29] N. Abdolhossein, H. Soheila, R. Farzaneh, M. R. Reza, Z. Maryam, K. Taghi, *J. Lumin.* **2015**, *157*, 104.

[30] S. Neelam, M. Gokara, B. Sudhamalla, D. G. Amooru, R. Subramanyam, *J. Phys. Chem. B* **2010**, *114*, 3005.

[31] Z. Ye-Zhong, C. Xiao-Xia, D. Jie, Z. Xiao-Ping, L. Yan-Xia, L. Yi, *Luminescence* **2008**, *23*, 150.

[32] N. Yongnian, L. Genlan, K. Serge, *Talanta* **2008**, *76*, 513.

[33] D. P. Ross, S. Subramanian, *Biochemistry* **1981**, *20*, 3096.

[34] H. Yan-Jun, Y. Ou-Yang, D. Chun-Mei, L. Yi, X. Xiao-He, *Biomacromolecules* **2010**, *11*, 106.

[35] S. Yuguang, L. Yangping, L. Wenbo, A. V. Frederick, L. Z. Jay, *RSC Adv.* **2014**, *4*, 47649.

[36] D. C. Carter, B. Chang, J. X. Ho, K. Keeling, Z. Krishnasami, *Eur. J. Biochem.* **1994**, *226*, 1049.

[37] J. Ghuman, P. A. Zunszain, I. Petitpas, A. A. Bhattacharya, M. Otagiri, S. Curry, *J. Mol. Biol.* **2005**, *353*, 38.

[38] Y. Yue, Y. Sun, Q. Dong, R. Liu, X. Yan, Y. Zhang, J. Liu, *Luminescence* **2016**, *31*, 671.

[39] K. P. Bijan, G. Narayani, M. Saptarshi, *J. Phys. Chem. B* **2015**, *119*, 13093.

[40] B. K. Paul, N. Ghosh, S. Mukherjee, *Langmuir* **2014**, *30*, 5921.

[41] S. Moumita, S. P. Shiv, K. M. Kalyan, *J. Lumin.* **2013**, *142*, 220.

[42] S. A. Mohd, A. Hamad, Al-Lohedan, *J. Lumin.* **2016**, *169*, 35.

[43] W. K. Surewicz, H. H. Mantsch, *Biochim. Biophys. Acta* **1988**, *952*, 115.

[44] W. Qi, H. Chuan-ren, M. Jiang, Z. Ying-yao, W. Jing, J. Chen, S. Jie-hua, *Spectrochim. Acta Mol. Biomol. Spectrosc.* **2016**, *156*, 155.

[45] Y. Yuanyuan, D. Qiao, Z. Yajie, L. Xiaoge, Y. Xuyang, S. Yahui, L. Jianming, *Spectrochim. Acta A* **2016**, *153*, 688.

[46] L. Stryer, R. P. Haugland, *Proc. Natl. Acad. Sci. U. S. A.* **1967**, *58*, 719.

[47] X. H. Wu, J. J. Liu, H. M. Huang, W. W. Xue, X. J. Yao, J. Jin, *Int. J. Biol. Macromol.* **2011**, *49*, 343.

[48] Y. H. Pang, L. L. Yang, S. M. Shuang, C. Dong, M. Thompson, *J. Photochem. Photobiol. B Biol.* **2005**, *80*, 139.

[49] M. Ishtikhar, S. Khan, G. Badr, A. O. Mohamed, R. K. Hasan, *Mol. BioSyst.* **2014**, *10*, 2954.

[50] S. Nahid, H. Saba, F. Foroozan, *Spectrochim. Acta Mol. Biomol. Spectrosc.* **2015**, *138*, 169.

[51] S. M. Kelly, N. C. Price, *Biochim. Biophys. Acta* **1997**, *1338*, 161.

[52] T. Wang, B. Xiang, Y. Wang, C. Chen, Y. Dong, H. Fang, M. Wang, *Colloids Surf., B* **2008**, *65*, 113.

[53] Y. Zhang, Y. Li, L. Dong, J. Li, W. He, X. Chen, Z. Hu, *J. Mol. Struct.* **2008**, *875*, 1.

[54] D. Li, B. Ji, H. Sun, *Spectrochim. Acta A* **2009**, *73*, 35.

How to cite this article: Pawar SK, Jaldappagari S. Probing the mechanism of interaction of metoprolol succinate with human serum albumin by spectroscopic and molecular docking analysis. *Luminescence*. 2017;00:1-10. doi: 10.1002/bio.3275